RIYA Final Report (2017)

Non-linear dynamics of wire rope isolators

Priy Ranjan, RIYA Scholar

Indian Institute of Technology Madras

Mentors

Prof. Rajendra Singh

Dr. Nick Mastricola

Helical wire rope isolator

Polycal wire rope isolator

THE OHIO STATE UNIVERSITY

Motivation

<u>Wire rope isolator applications</u>

- Aerospace industry
- Civil structures
- Military

<u>Primary advantages</u>

- Isolation in 6 degrees of freedom [1]
- Wire ropes resist aging and corrosion, and can work at higher temperatures [2]

<u>Prior work</u>

a. The existing models are mostly empirical and do not adequately investigate the non-linear dynamics of such systems. b. Limitation of Prior literature - limited experimental work. (See Appendix D for a summary.)

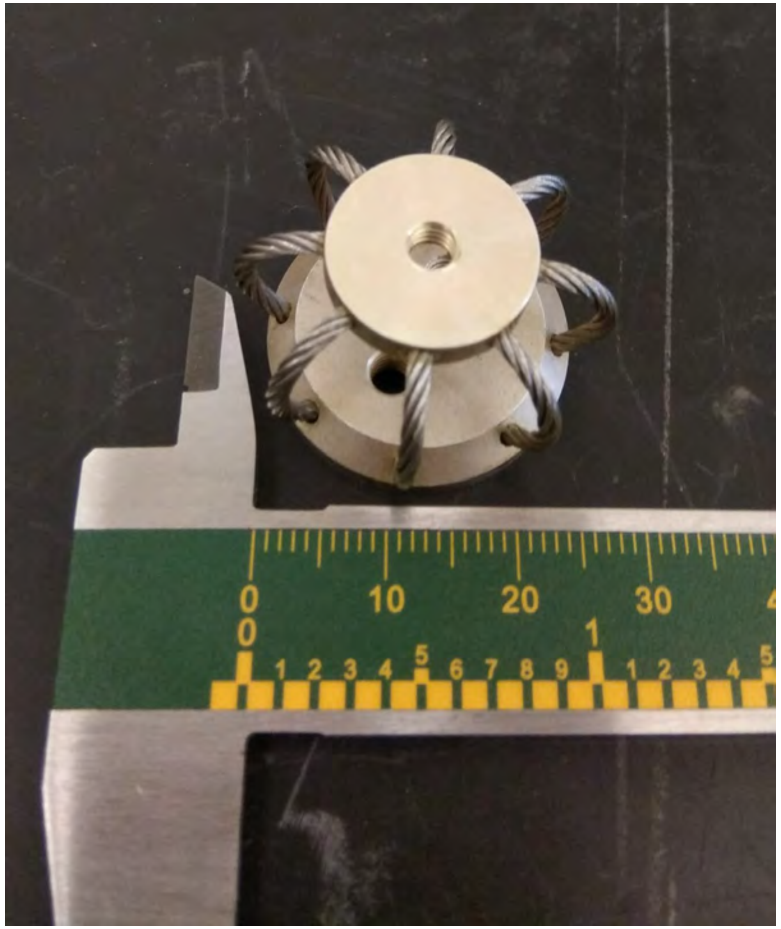

Fig. 1: Polycal isolator used in our experiments

Sources: [1] G. F. Demetriades et al., *"Study of wire rope systems for seismic protection of equipment in buildings"*, Engg. Stuct vol. 15 no. 5, 1993

[2] P.S. Balaji et al., *"Experimental investigation on the hysteresis behavior of the wire rope isolators"*, JMST vol. 29 no. 4 pp. 1527-1536, 2015

Objectives

- Characterize the static behavior of wire rope isolators behavior (load-deflection curves and hysteresis under quasi-static loads)
- Investigate the dynamic (modal) behavior of a system with 2 wire rope isolators.

Scope

- Helical wire rope isolators
- Quasi-static and impulse excitation experiments
- Non-linear models of static behavior
- Modal experiments (about an operating point)

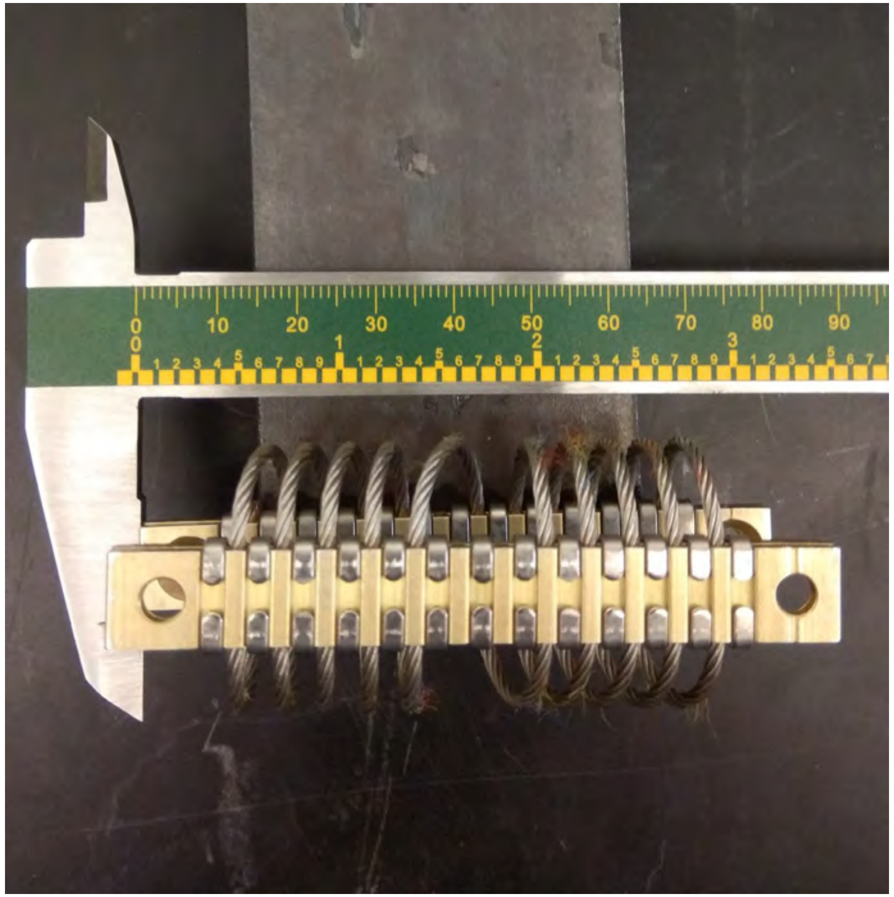

Fig. 2: Helical isolator used in our static and dynamic experiments

Quasi-static experiment

Fig. 3: Setup

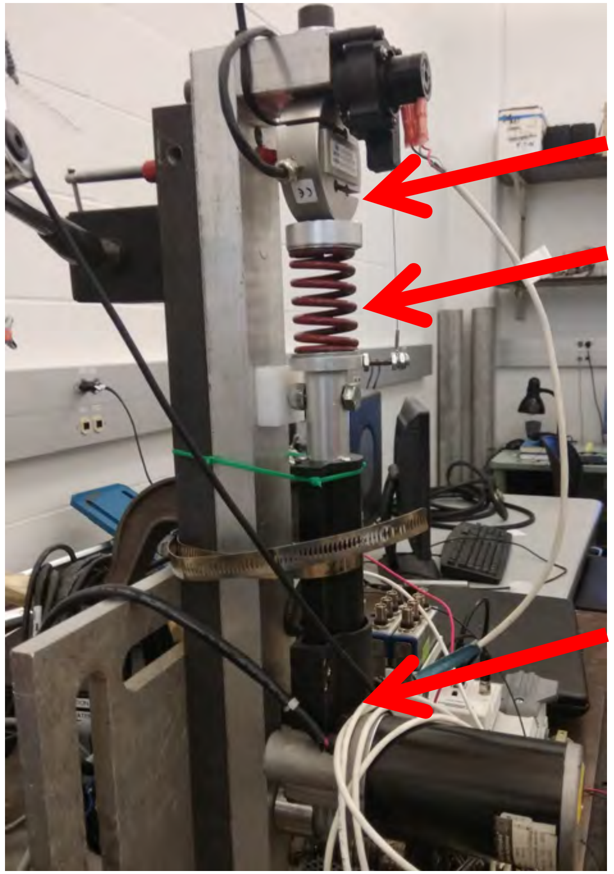

Load Cell

Spring

Power screw

Methodology

Static force-displacement curves for 3 wire rope isolators (labeled A, B, and C) obtained:

- Load and unload using a power-screw
- Measure the force using a load cell
- Measure the displacement using a string potentiometer

[Video]

Fig. 4a-b: Configurations

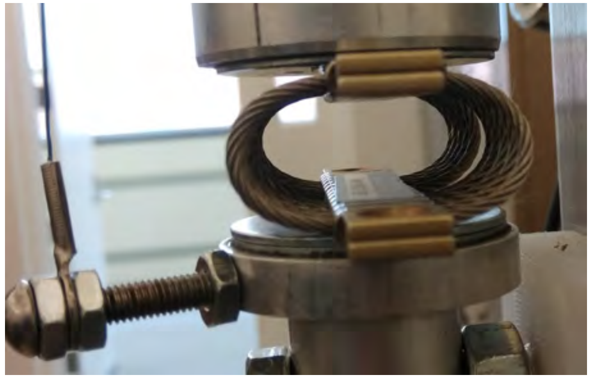

Normally loaded

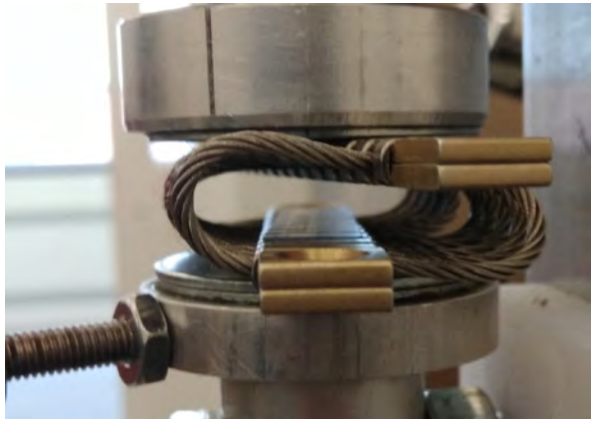

Twisted during loading

The Ohio State University

Measured load-deflection curves (I)

Tension-compression

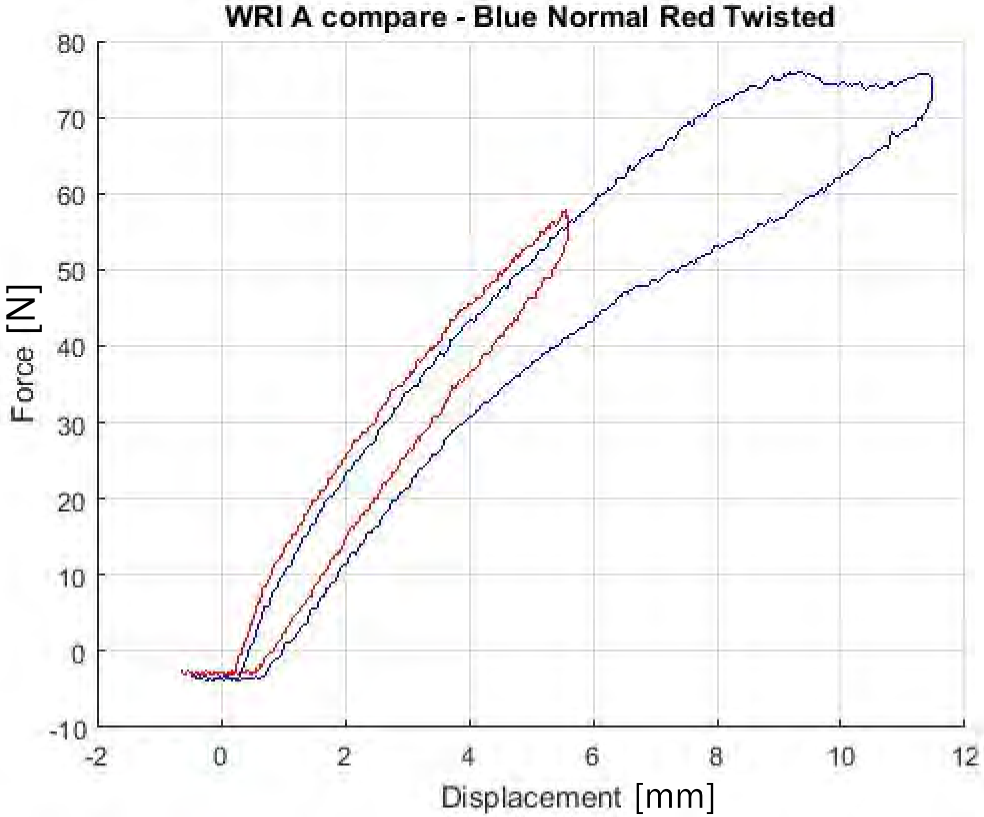

Fig. 5: Force-displacement curves of isolator A in normal and twisted configurations.

Tension-compression

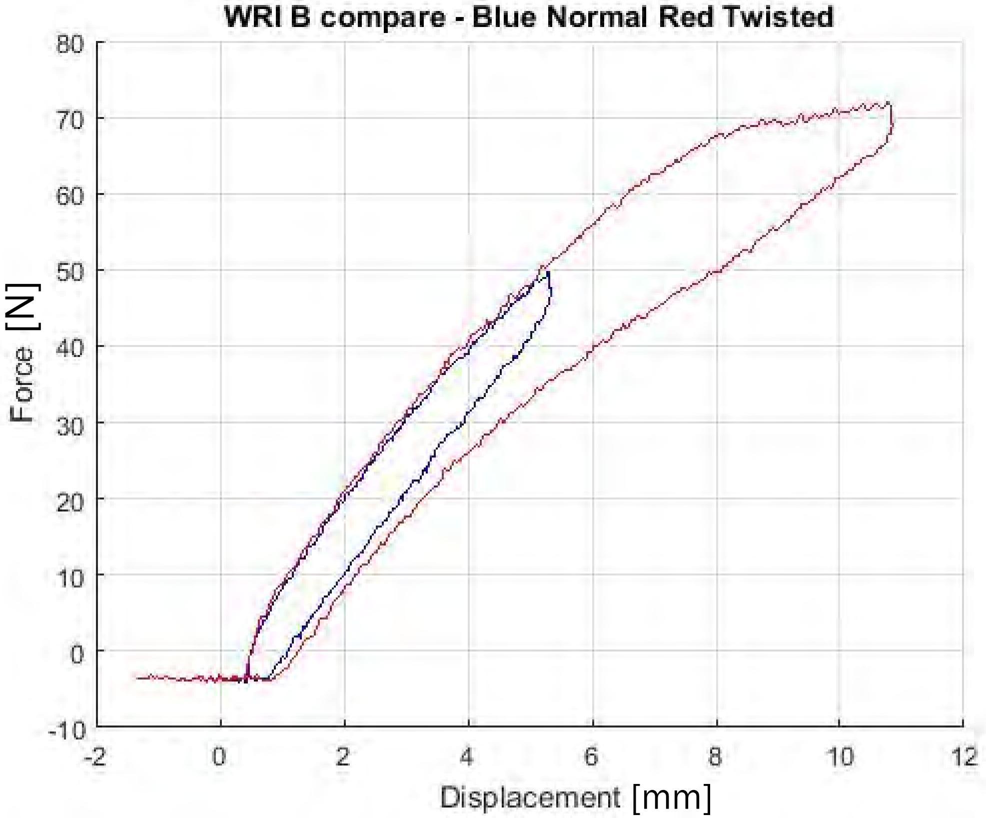

Fig. 6: Force-displacement curves of isolator B in normal and twisted configurations.

Measured load-deflection curves (II)

Tension-compression

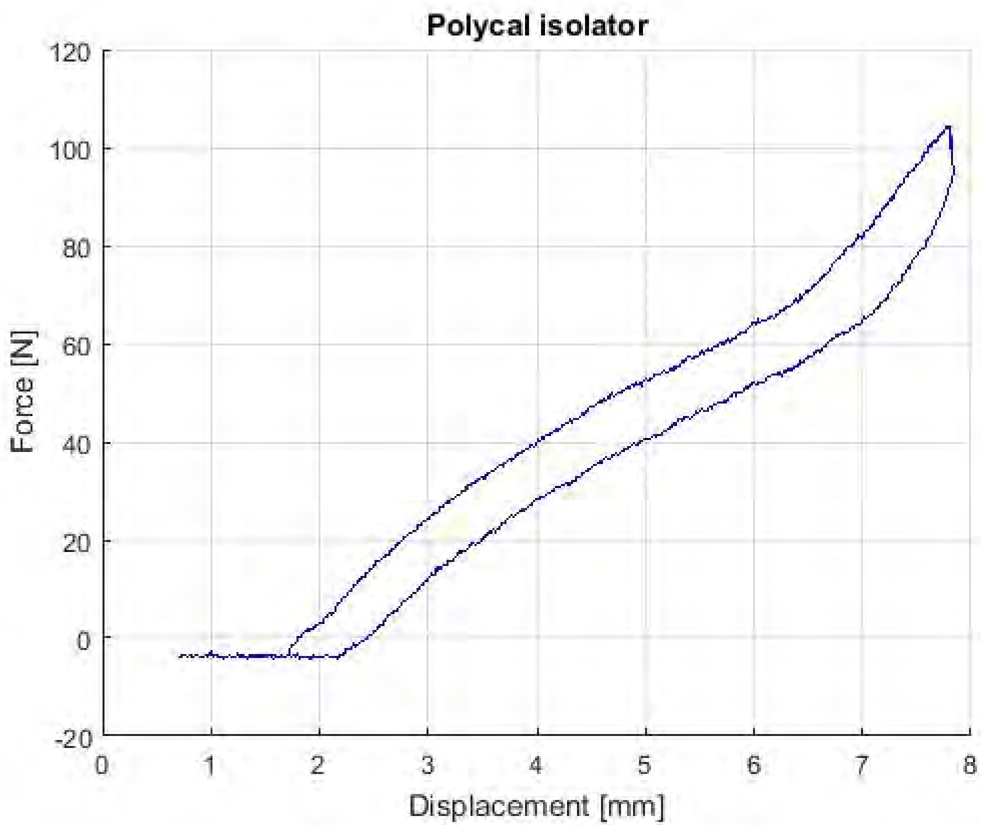

Fig. 7: Force-displacement curves of a polycal isolator C

Polycal isolators exhibit softening-hardening behavior under loading

The force-deflection curve can be modeled using a modified Buoc-Wen model (Ni et al. 1999)

Load-deflection curve-fits I (Figs. 8 & 9)

a = friction coefficient (constant)

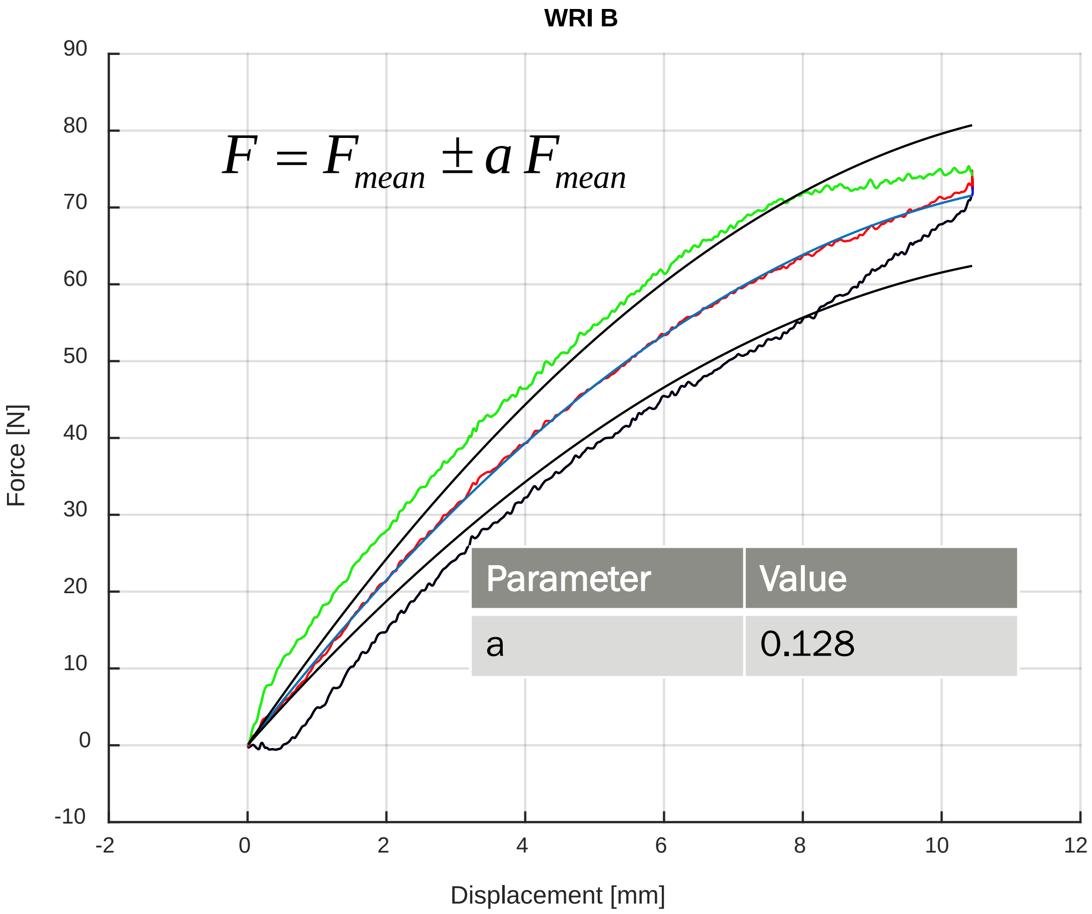

Parameter	Value
a	0.128

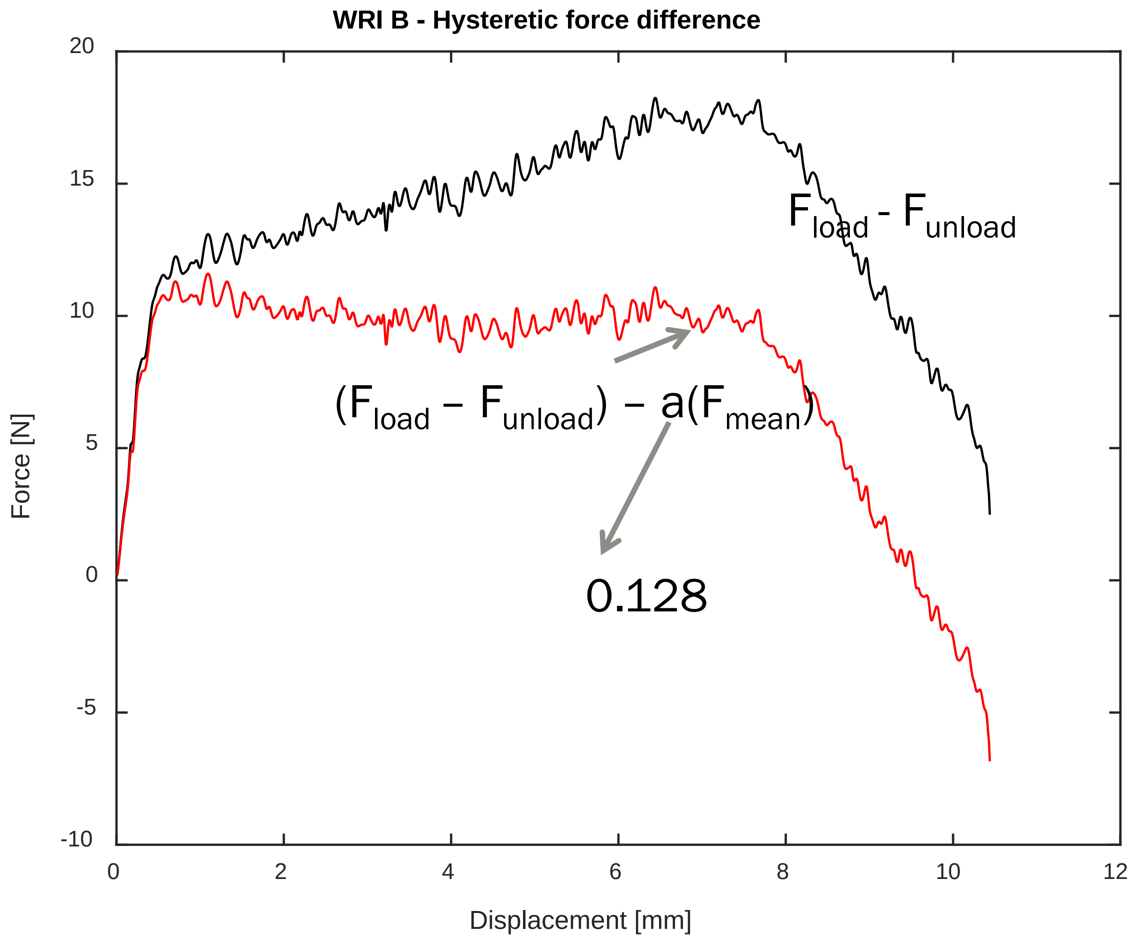

The Ohio State University

Load-deflection curve-fits II (Fig. 10)

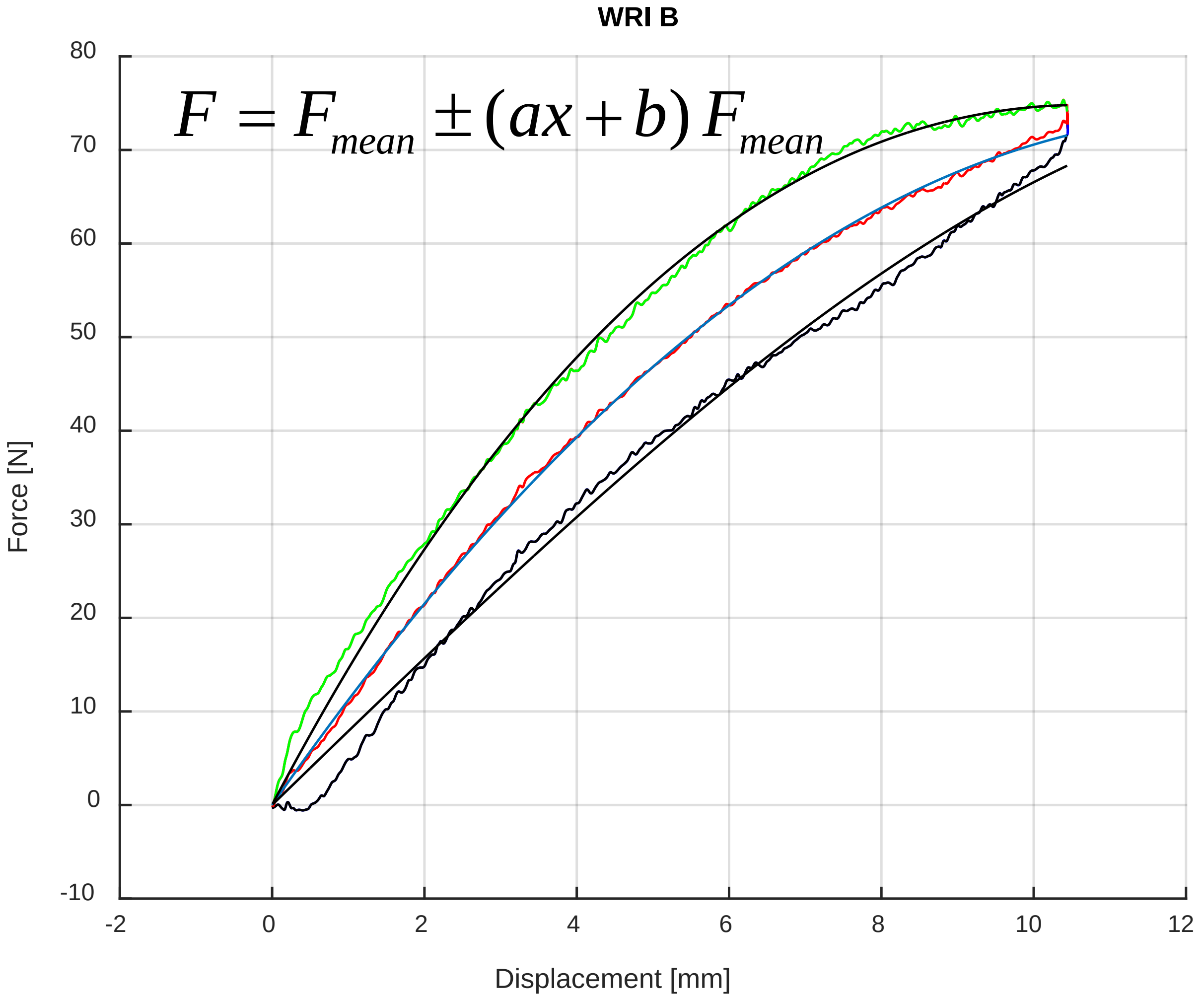

(ax+b) = friction coefficient (linear function of x)

Using least-square error optimization,
Optimal values (a & b) are obtained.

Parameter	Value
a	-0.026
b	0.32

Observation: The friction formulation (ax+b) seems to fit well.

Measured load-deflection curves in shear (Figs. 11 and 12)

Shear

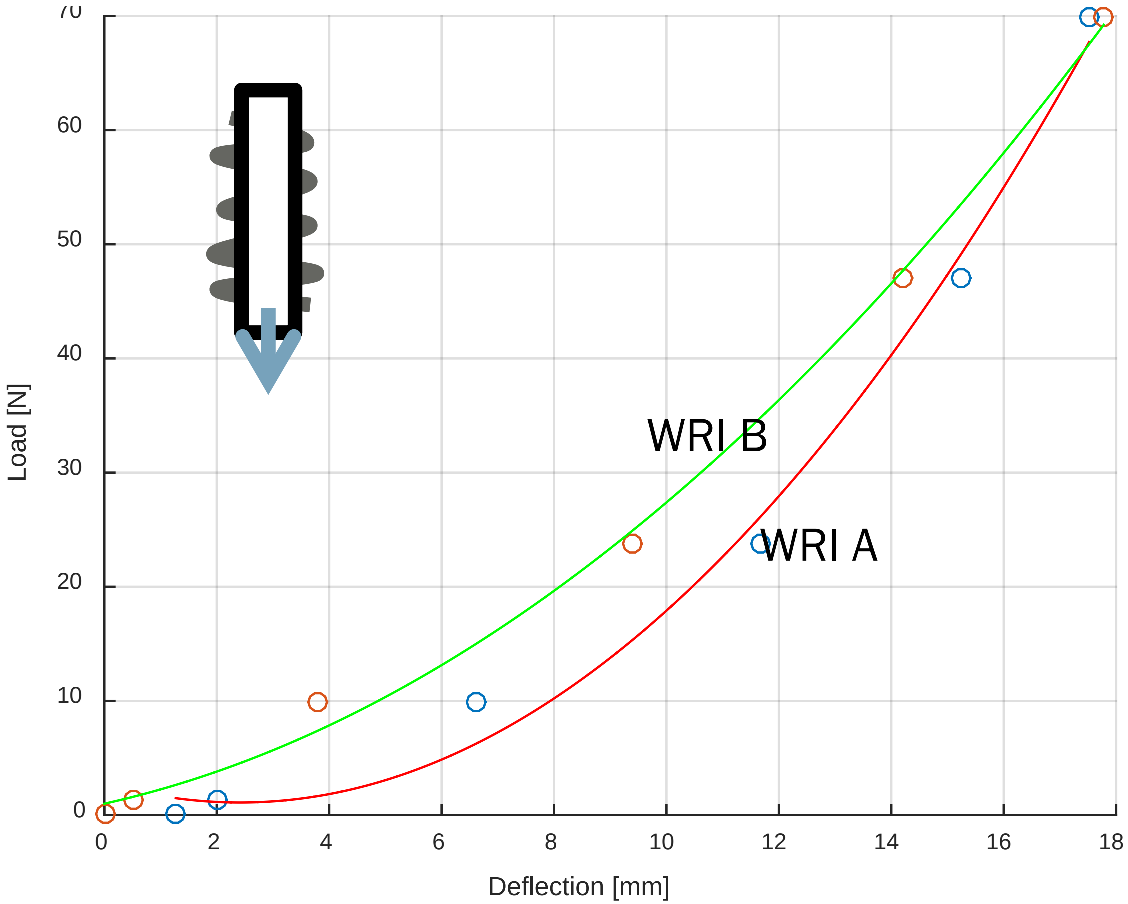

Shear

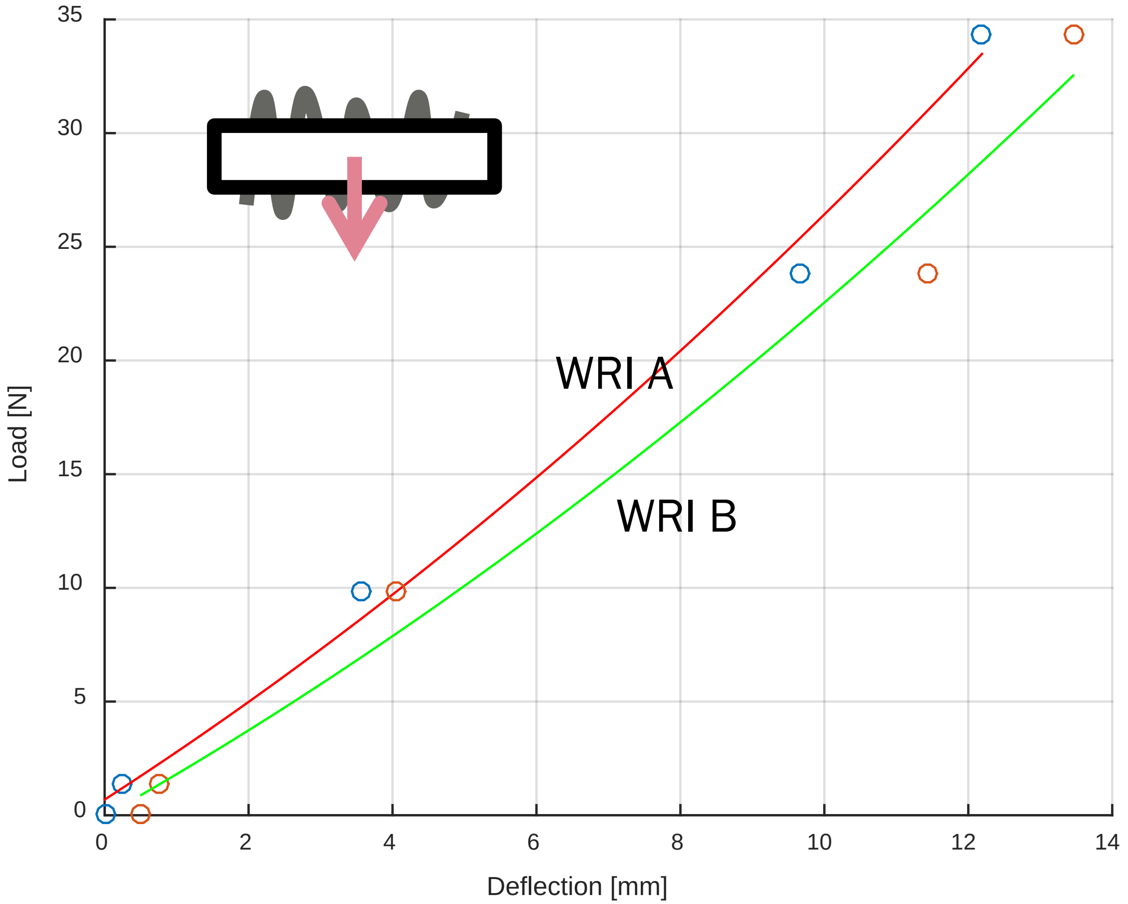

Comparison with prior literature (Figs. 13-15)

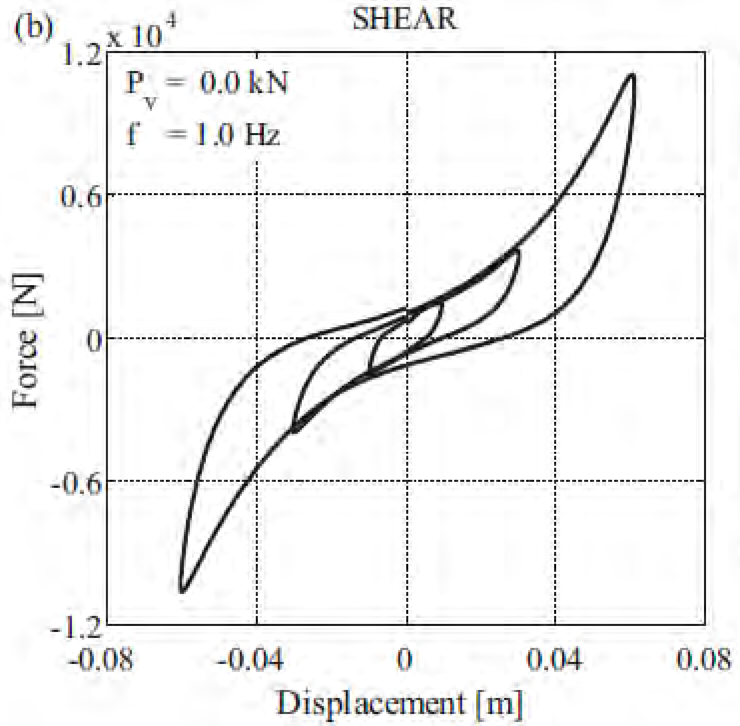

Source: Viana et al. (2017)

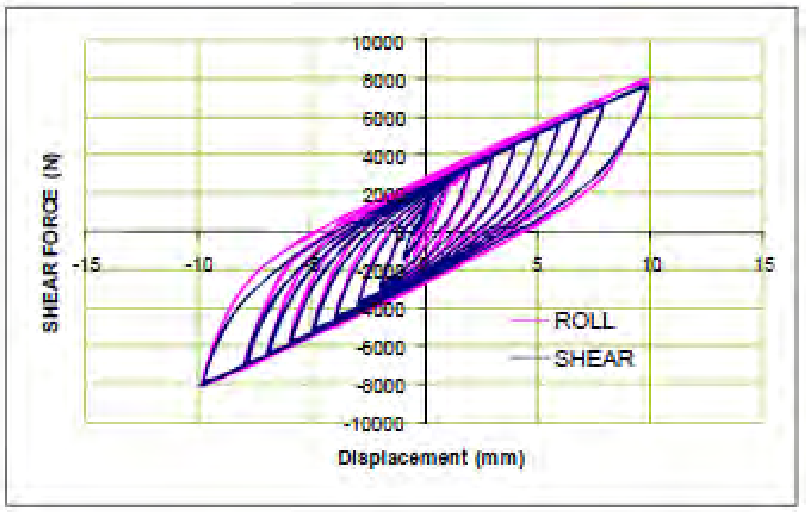

Figure 4 Shear cycles of a WR28-400-08

Source: Paolacci and Giannini. (2008)

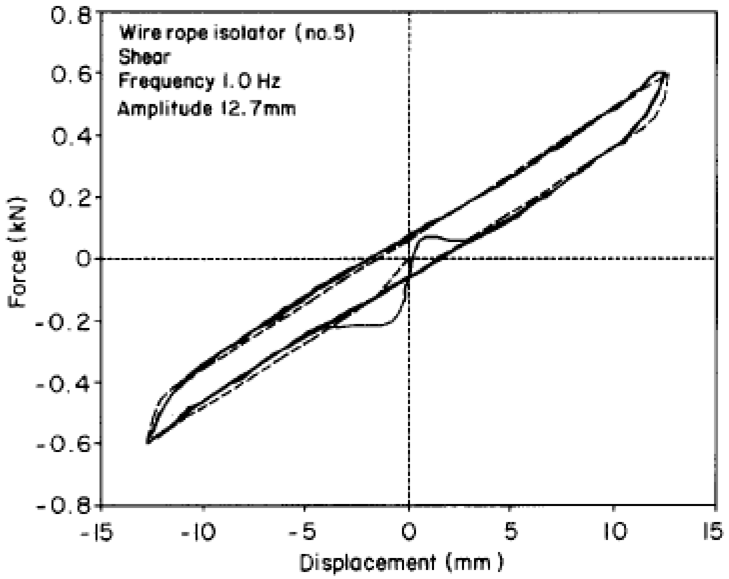

Source: Demetriades et al. (1992)

Observation: Shear force-deflection curves show either hardening or linear behavior during loading

The Ohio State University

Measured load-deflection curves in Pitch Mode (Fig. 16)

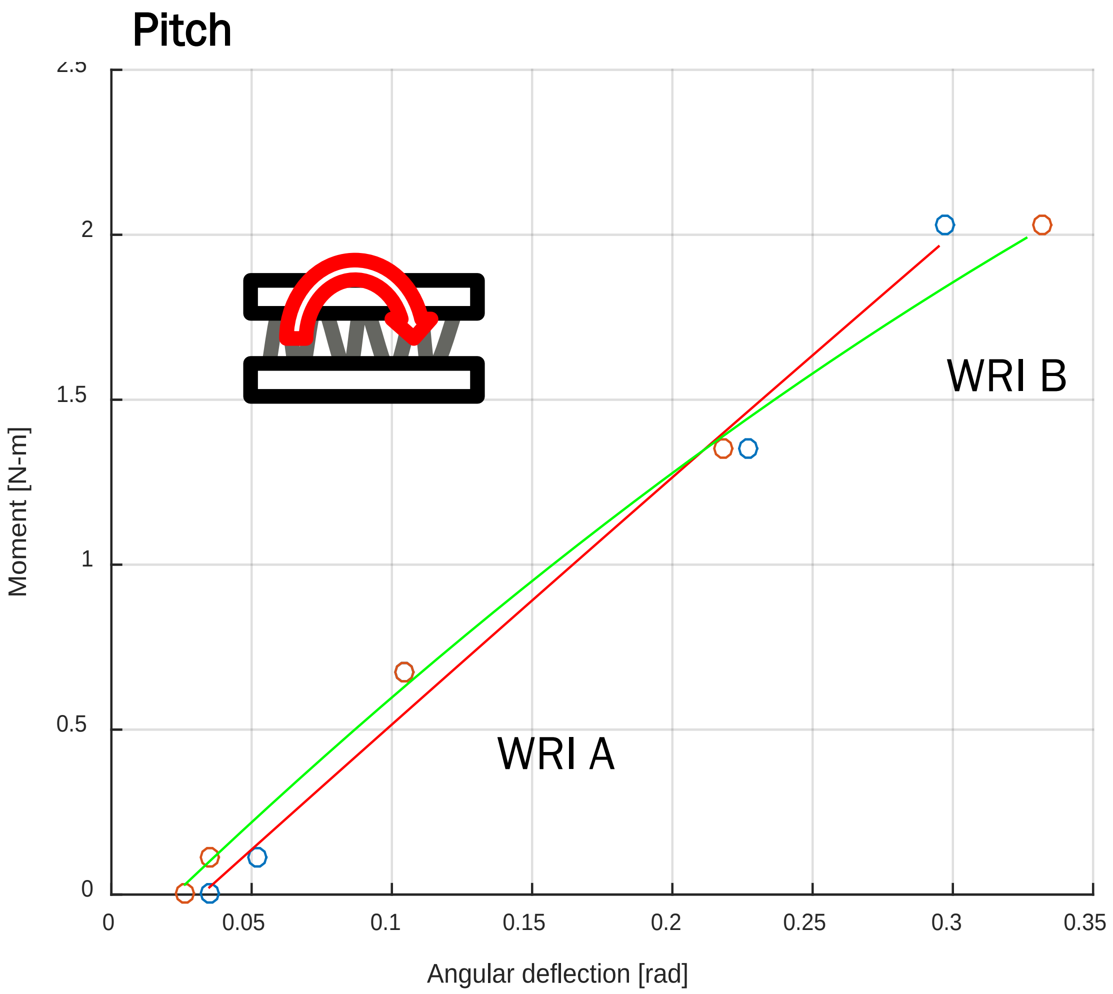

Observation: The angular stiffness in the pitch mode has not been reported in the previous literature

Dynamic experiment (designed in the 2DOF system configuration)

Setup (Fig. 17)

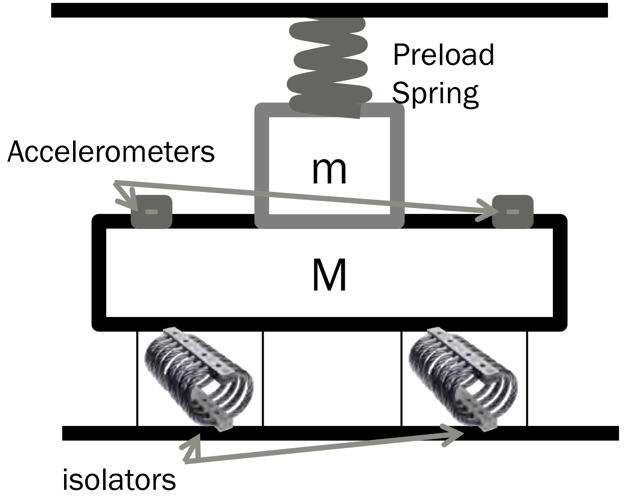

Methodology

- System is excited using an instrumented impulse hammer
- Responses are measured using 2 tri-axial accelerometers (on mass M)
- Signals are acquired and processed using LMS system

Configurations (Figs. 18-19a,b)

Mass M only

Mass M and m, Preload spring

Mass M, Preload spring

Assumption

- Linear system around the operating point

2DOF model of undamped, unforced isolation system (Fig. 20)

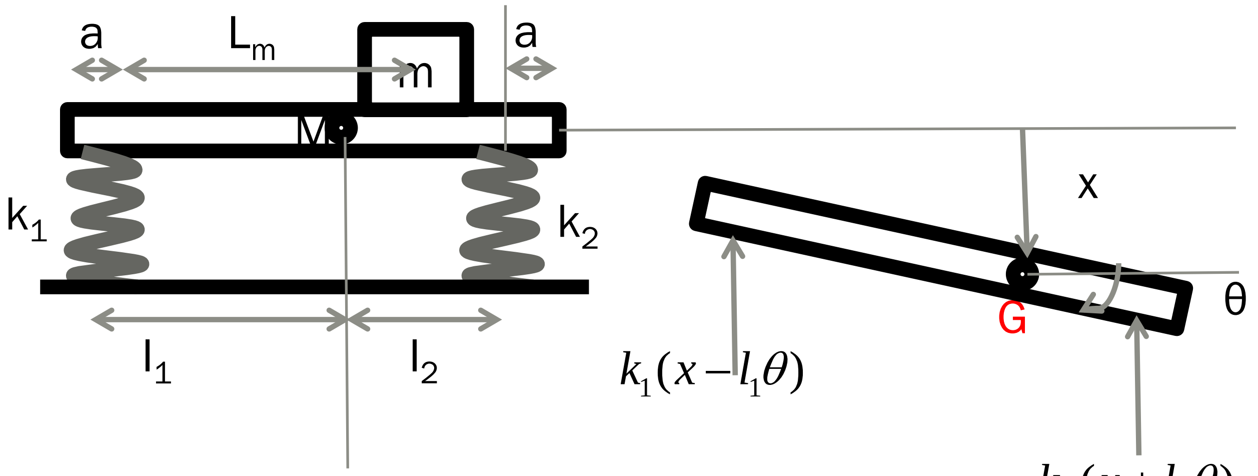

k_1 & k_2 : Spring stiffness

Assumptions:

- Linear system
- Isolators represented by 2 springs in parallel.
- Motions given by translation (x) and pitch (θ) about the CG (G)
- Asymmetry in mass is modeled by a concentrated mass m at distance L_m from k_1

Force equilibrium in the vertical direction:

$$(M+m)\ddot{x} + k_1(x - l_1\theta) + k_2(x + l_2\theta) = 0$$

Moment equilibrium about G:

$$J\ddot{\theta} - k_1(x - l_1\theta)l_1 + k_2(x + l_2\theta)l_2 = 0$$

$$\begin{bmatrix} M+m & 0 \\ 0 & J \end{bmatrix} \begin{Bmatrix} \ddot{x} \\ \ddot{\theta} \end{Bmatrix} + \begin{bmatrix} k_1 + k_2 & -k_1 l_1 + k_2 l_2 \\ -k_1 l_1 + k_2 l_2 & k_1 l_1^2 + k_2 l_2^2 \end{bmatrix} \begin{Bmatrix} x \\ \theta \end{Bmatrix} = \begin{Bmatrix} 0 \\ 0 \end{Bmatrix}$$

Measured accelerances: Fig. 21

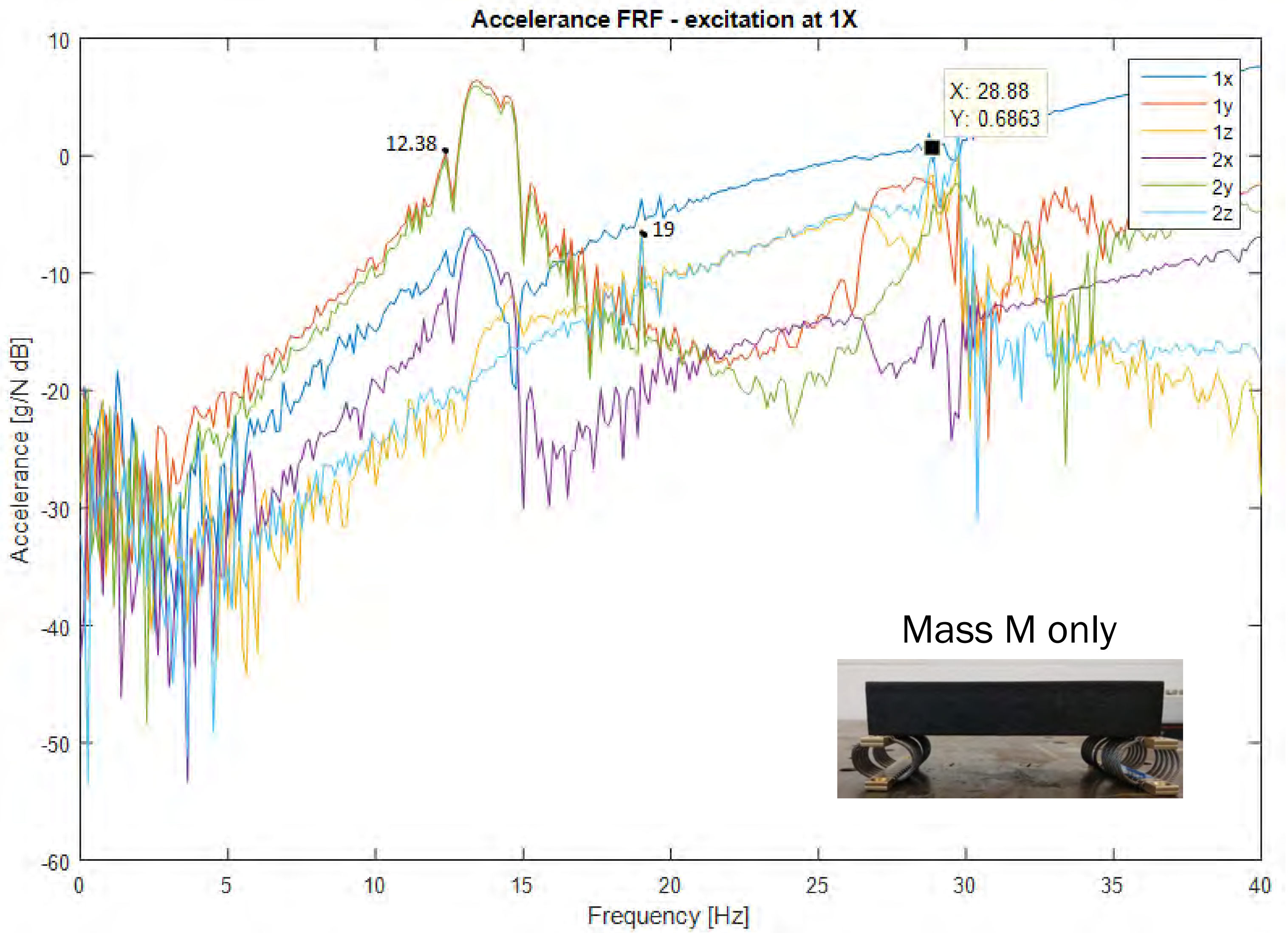

2DOF system eigenvalue problem yields:

- 13.8 Hz
- 22 Hz

Observations:

1. Although resonant peaks in measurements are close to calculated frequencies, additional modes are also seen
2. Extend the analytical model to 6DOF system

6DOF model of undamped, unforced isolation system (Fig. 22)

See Appendix B and C for more details

Schematic of the system

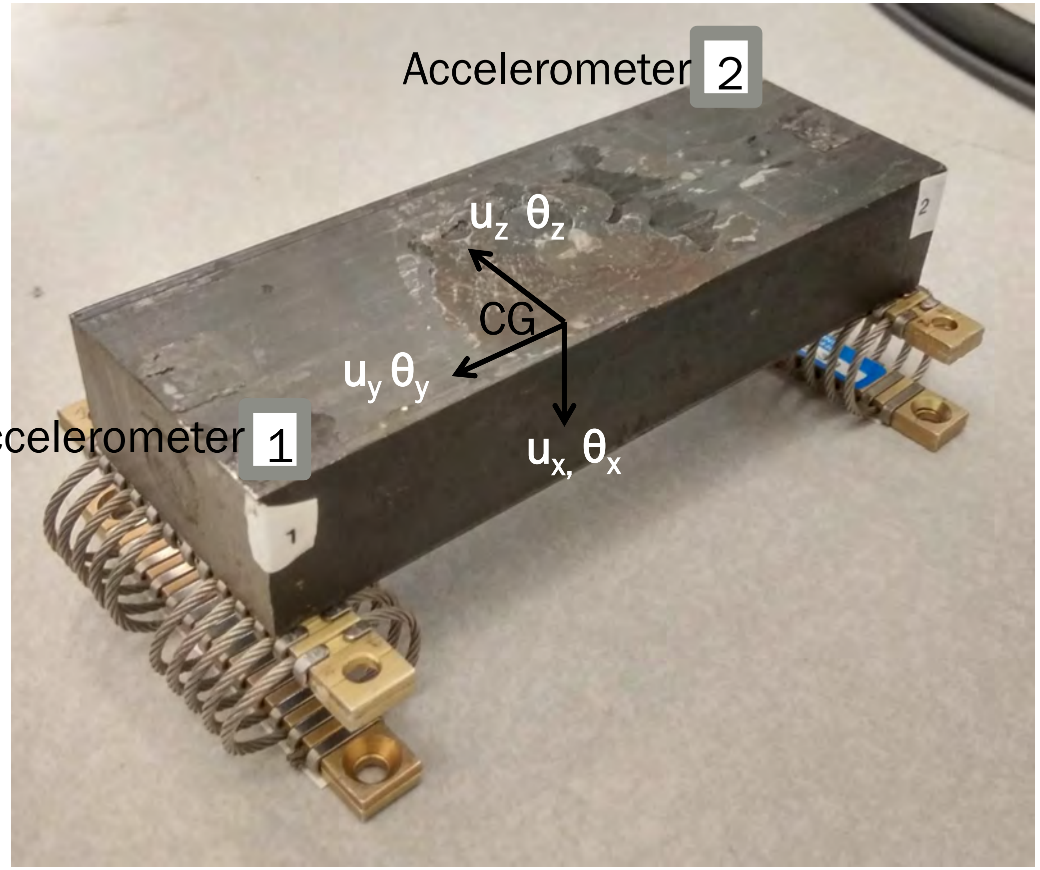

The displacement of point 1,

$$u_1 = \begin{Bmatrix} u_x - l_y\theta_z - l_z\theta_y \\ u_y - l_x\theta_z + l_z\theta_x \\ u_z + l_x\theta_y + l_y\theta_x \end{Bmatrix}$$

And, displacement point 2,

$$u_2 = \begin{Bmatrix} u_x + l_y\theta_z + l_z\theta_y \\ u_y - l_x\theta_z - l_z\theta_x \\ u_z + l_x\theta_y - l_y\theta_x \end{Bmatrix}$$

u_i = displacement in the i-direction (x, y, z)

θ_i = angular displacement about the i-axis (x, y, z)

Analytical eigensolutions – 6DOF model (Fig. 23) see Appendix C

Configuration

Mass M and m,
Preload spring

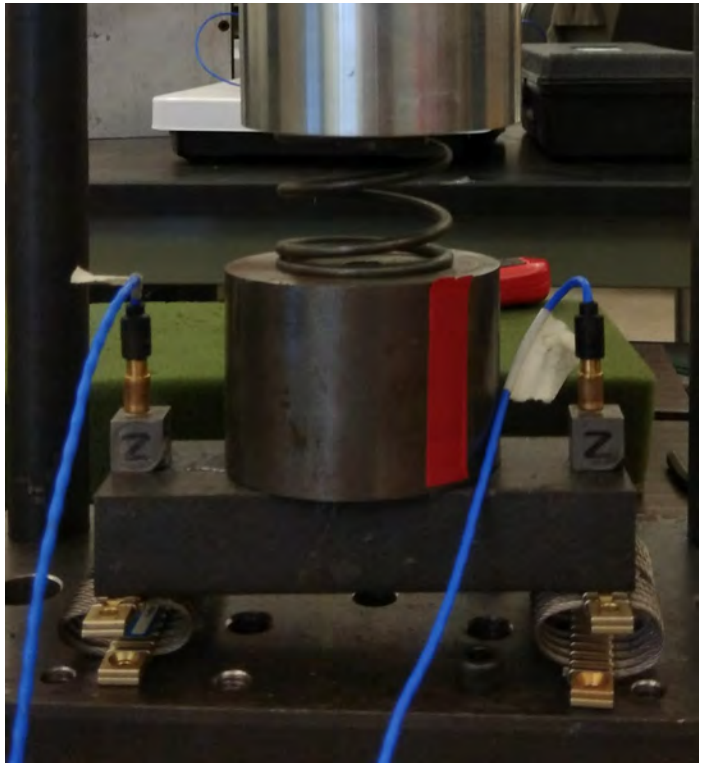

Eigensolutions yield:

Natural frequencies (in Hz)

$$\omega_i = \begin{Bmatrix} 28.8 \\ 18.8 \\ 6.4 \\ 4.3 \\ 5.3 \\ 23.4 \end{Bmatrix}$$

Modal matrix

$$\Psi = \begin{bmatrix} 0 & 0 & 0 & 0 & 0 & 1.00 \\ 0 & -0.02 & -0.06 & 0.07 & 0 & 0 \\ 0 & 0 & 0.10 & 0.05 & 0 & 0 \\ 0 & 0 & -0.02 & -0.02 & -1.00 & 0 \\ -0.99 & -0.22 & -0.84 & -0.58 & 0 & 0 \\ -0.11 & 0.98 & -0.53 & 0.81 & 0 & 0 \end{bmatrix}$$

Measured accelerances (Fig. 24)

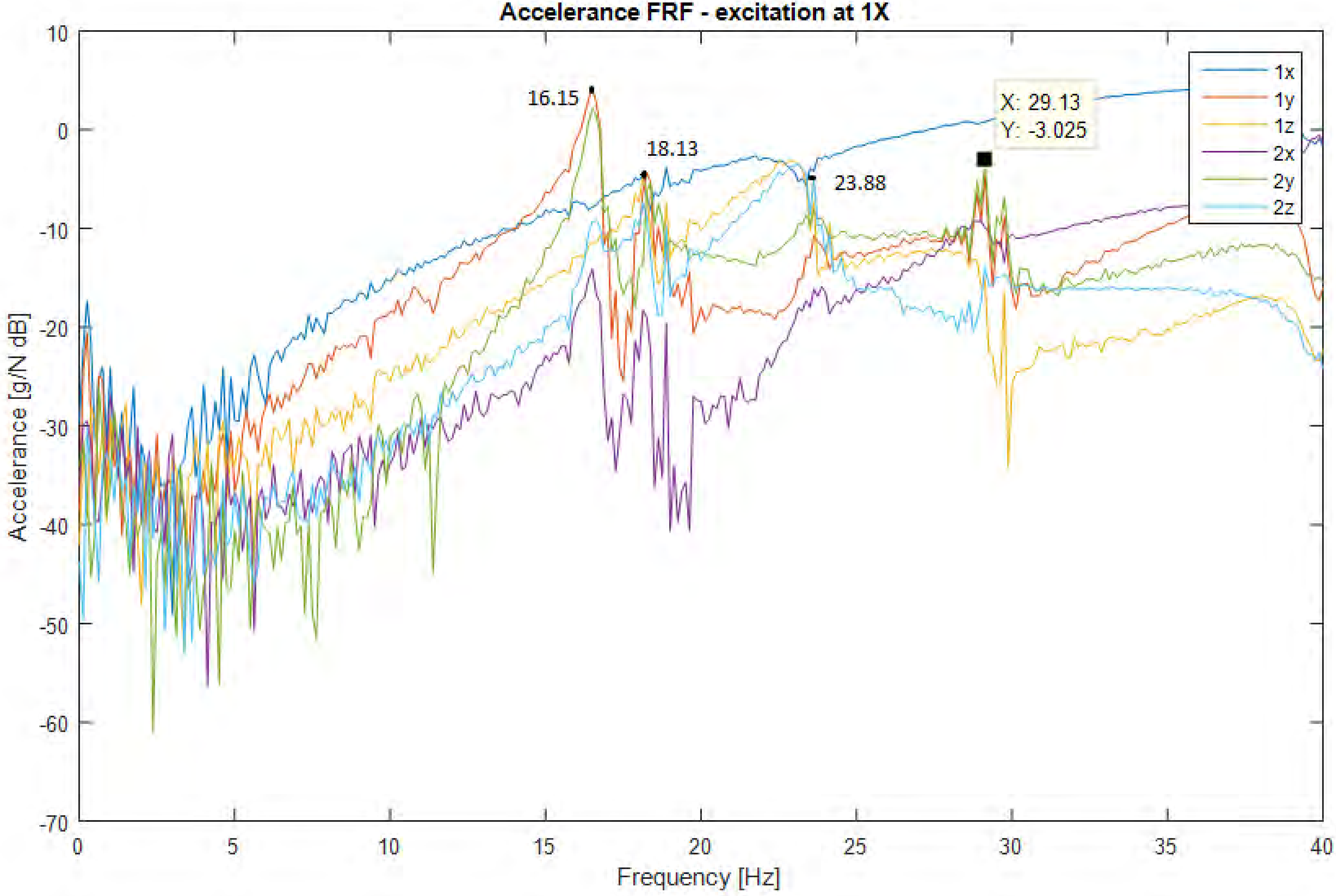

Observations:

1. Peaks in measurements are close to the calculations (natural frequencies from 15 Hz to 40 Hz)
2. Coherence is poor below 10 Hz (possibly due to high damping)
3. As a result, peaks are not observed up to 10 Hz
4. Damping ratio for resonance around 16 Hz: 1.5%

Conclusion

1. Investigated the non-linear dynamics of the wire rope isolators in the context of existing literature.

2. Correlated measurements and calculations. Identified several interesting new observations.

3. Identified some consequences of incorporating non-linearities in the design of isolation systems

4. Outlined new work on wire rope isolators.

Fig. 25 Application of wire-rope isolators in quad-rotors

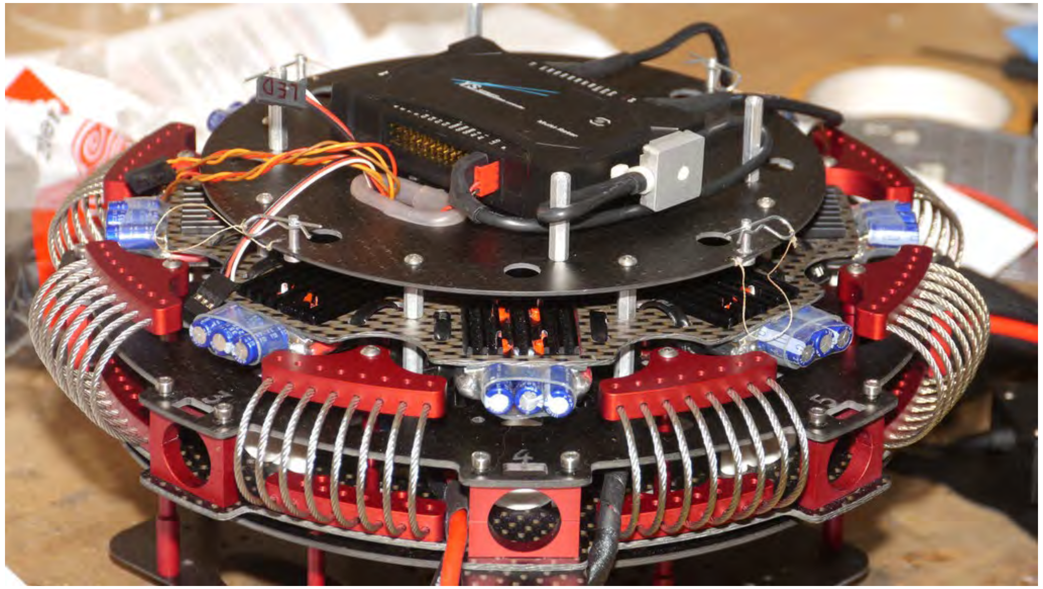

Appendix A: Topics and lessons learned

- Non-linear dynamics
- Vibration isolation
- Real-life devices
- Modal analysis & testing

- *Design of experiments*
- *Experimental work (under the supervision of mentor)*
- *Static & dynamic experiments*
- *Data processing*
- *Interpretation of results*
- *Best practices in presenting technical work*

Appendix B: 6 DOF model equations (Fig. 26)

Schematic of the system

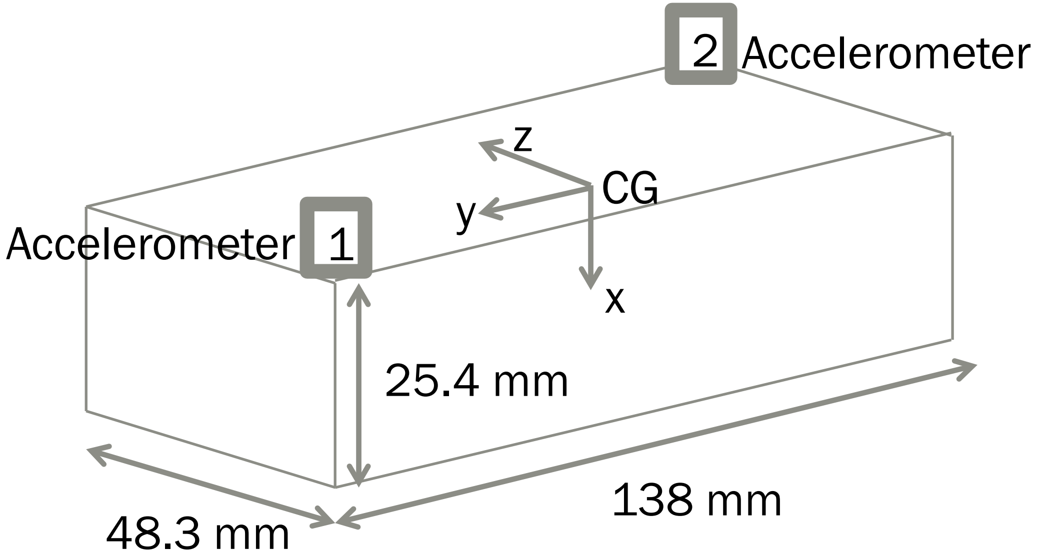

0

Force equilibrium in x, y and z directions:-

$$M\ddot{u}_x - k_{1x}(l_y\theta_z - u_x + l_z\theta_y) + k_{2x}(u_x + l_y\theta_z + l_z\theta_y) = 0$$
$$M\ddot{u}_y + k_{1y}(u_y - l_x\theta_z + l_z\theta_x) - k_{2y}(l_x\theta_z - u_y + l_z\theta_x) = 0$$
$$M\ddot{u}_z + k_{1z}(u_z + l_x\theta_y + l_y\theta_x) + k_{2z}(u_z + l_x\theta_y - l_y\theta_x) = 0$$

Moment equilibrium about x, y and z directions:-

$$J_x\ddot{\theta}_x + k_{1z}l_y(u_z + l_x\theta_y + l_y\theta_x) - k_{2z}l_y(u_z + l_x\theta_y - l_y\theta_x) + k_{1y}l_z(u_y - l_x\theta_z + l_z\theta_x) + k_{2y}l_z(l_x\theta_z - u_y + l_z\theta_x) = 0$$
$$J_y\ddot{\theta}_y + k_{1z}l_x(u_z + l_x\theta_y + l_y\theta_x) + k_{2z}l_x(u_z + l_x\theta_y - ly\theta_x) + k_{2x}l_z(u_x + l_y\theta_z + l_z\theta_y) + k_{1x}l_z(l_y\theta_z - u_x + l_z\theta_y) = 0$$
$$J_z\ddot{\theta}_z - k_{1y}l_x(u_y - l_x\theta_z + l_z\theta_x) + k_{2x}l_y(u_x + l_y\theta_z + l_z\theta_y) + k_{2y}l_x(l_x\theta_z - u_y + l_z\theta_x) + k_{1x}l_y(l_y\theta_z - u_x + l_z\theta_y) = 0$$

Appendix C: Eigenvalue problem formulation

Mass matrix

$$\begin{bmatrix} M & 0 & 0 & 0 & 0 & 0 \\ 0 & M & 0 & 0 & 0 & 0 \\ 0 & 0 & M & 0 & 0 & 0 \\ 0 & 0 & 0 & J_x & 0 & 0 \\ 0 & 0 & 0 & 0 & J_y & 0 \\ 0 & 0 & 0 & 0 & 0 & J_z \end{bmatrix}$$

Dimension = 6
M = mass of the system
i = x, y, z
J_i = moment of inertia about i-axis
u_i = translation in the i^{th} direction
θ_i = angular displacement about the i-axis
k_{1i} = stiffness of B in the i^{th} direction
k_{2i} = stiffness of A in the i^{th} direction
$k_{\theta y1}$ and $k_{\theta y2}$ = angular stiffness about y-axis for isolator B & A
l_i = distance between CG and points 1 and 2 along i-axis

Generalized displacement vector

$$\begin{Bmatrix} u_x \\ u_y \\ u_z \\ \theta_x \\ \theta_y \\ \theta_z \end{Bmatrix}$$

Stiffness matrix

$$\begin{bmatrix} k_{1x}+k_{2x} & 0 & 0 & 0 & -k_{1x}l_z+k_{2x}l_z & -k_{1x}l_y+k_{2x}l_y \\ 0 & k_{1y}+k_{2y} & 0 & k_{1y}l_z-k_{2y}l_z & 0 & -k_{1y}l_x-k_{2y}l_x \\ 0 & 0 & k_{1z}+k_{2z} & k_{1z}l_y-k_{2z}l_y & k_{1z}l_x+k_{2z}l_x & 0 \\ 0 & k_{1y}l_z-k_{2y}l_z & k_{1z}l_y-k_{2z}l_y & k_{1z}l_y{}^2+k_{2z}l_y{}^2+k_{1y}l_z{}^2+k_{2y}l_z{}^2 & k_{1z}l_yl_x-k_{2z}l_yl_x & -k_{1y}l_zl_x+k_{2y}l_zl_x \\ k_{2x}l_z-k_{1x}l_z & 0 & k_{1z}l_x+k_{2z}l_x & k_{1z}l_xl_y-k_{2z}l_xl_y & k_{1z}l_x{}^2+k_{2z}l_x{}^2+k_{2x}l_z{}^2+k_{1x}l_z{}^2+k_{\theta y1}+k_{\theta y2} & k_{2x}l_zl_y+k_{1x}l_zl_y \\ k_{2x}l_y-k_{1x}l_y & -k_{1y}l_x-k_{2y}l_x & 0 & -k_{1y}l_xl_z+k_{2y}l_xl_z & k_{2x}l_yl_z+k_{1x}l_yl_z & k_{1y}l_x{}^2+k_{2x}l_y{}^2+k_{2y}l_x{}^2+k_{1x}l_y{}^2 \end{bmatrix}$$

Appendix D: List of References (see next slide for a summary)

1. Balaji, P. S. et al (2015). Experimental investigation on the hysteresis behavior of the wire rope isolators. *Journal of Mechanical Science and Technology*, *29*(4), 1527.
2. Gerges, R. R. (2008). Model for the force–displacement relationship of wire rope springs. *Journal of Aerospace Engineering*, *21*(1), 1-9.
3. Ko, J. M. et al (1992). Hysteretic behavior and empirical modeling of a wire-cable vibration isolator.
4. Ni, Y. Q. et al (1999). Modelling and identification of a wire-cable vibration isolator via a cyclic loading test. *Proceedings of the Institution of Mechanical Engineers, Part I: Journal of Systems and Control Engineering*, *213*(3), 163-172.
5. Weimin, C. et al (1997). Research on ring structure wire-rope isolators. *Journal of materials processing technology*, *72*(1), 24-27.
6. Barbieri, N. et al (2016). Nonlinear dynamic analysis of wire-rope isolator and Stockbridge damper. *Nonlinear Dynamics*, *86*(1), 501-512.
7. Gerges, R. R., & Vickery, B. J. (2005). Design of tuned mass dampers incorporating wire rope springs. *Engineering Structures*, *27*(5), 653-661.
8. Pagano, S., & Strano, S. (2013). Wire rope springs for passive vibration control of a light steel structure. *WSEAS Trans. Appl. Theor. Mech*, *8*(3), 212-222.
9. Peifer, M. et al (2003). Non-parametric identification of non-linear oscillating systems. *Journal of sound and vibration*, *267*(5), 1157-1167.
10. Demetriades, G. F. et al (1993). Study of wire rope systems for seismic protection of equipment in buildings. *Engineering structures*, *15*(5), 321-334.
11. Di Massa, G. et al(2013). Sensitive equipment on WRS-BTU isolators. *Meccanica*, *48*(7), 1777-1790.
12. Paolacci, F., & Giannini, R. (2008). Study of the effectiveness of steel cable dampers for the seismic protection of electrical equipment. In *Proceedings of 14th World Conference on Earthquake Engineering* (pp. 12-17).
13. Tinker, M. L., & Cutchins, M. A. (1992). Damping phenomena in a wire rope vibration isolation system. *Journal of Sound and Vibration*, *157*(1), 7-18.
14. Vaiana, N., et al (2017). Wire rope isolators for seismically base-isolated lightweight structures: Experimental characterization and mathematical modeling. *Engineering Structures*, *140*, 498-514.

Summary of Literature Survey

Author (Journal, Year)	Topic	Comments
Ni et al. (JSV, 1999)	Modelling & identification of wire cable isolator	Modified Buoc-Wen model; Shear, roll and compression/tension
Gerges (JAE, 2008)	Model for force-displacement relation of wire rope isolator	Stiffness as summation of strand stiffness; compression/tension
Pagano & Strano (WSEAS, 2001)	Wire rope springs for passive vibration control	SDOF dynamic model; compression/tension
Demetriades et al. (Engg. Struct., 1993)	Wire rope systems for equipment seismic protection	Buoc-wen static model; 3DOF dynamic model
Wang et al. (Hindwani, 2014)	Dynamic behavior of O-type wire cable isolator	Assumes SDOF in each direction; compression/tension, shear and roll
Paolacci et al. (Conf. Earthquake Engg., 2008)	Effectiveness of steel cable dampers for seismic protection	4DOF dynamic model; compression/tension; shear and roll

Static | Dynamic Unidirectional | Dynamic Multi-directional